Electronic Supplementary Material (ESI) for Dalton Transactions.

Interconversion between Pd_3L_2 trigonal prism and Pd_6L_8 cube via anion exchange: binding affinity of monoatomic vs. polyatomic anions

Haeri Lee,[a,*] Jihoon Han[b] Dongwon Kim[b] and Ok-Sang Jung[b,*]

[a]Department of Chemistry, Hannam University, Daejeon 34054, Korea

[b]Department of Chemistry, Pusan National University, Busan 46241, Korea

Refinement details

Highly disordered solvate molecules were squeezed out by Platon. The equivalent estimation for squeezed solvents were performed by integration for ^{1}H NMR spectra, TG analyses, and elemental analyses. CIFs contain the detailed squeeze information. Most disagreeable reflections were omitted by OMIT instruction.

For 2065305, 2 structures for DMF and 1 structure for 1,4-dioxane are sharing the same position and refined as PART 1, 2, and 3 as suggested occupancies. The structure was refined with TWIN instruction.

For 2065306, this structure is refined as a 2-component inversion twin.

For 2065307, to obtain better diffraction data in lower angle, high angle data could not be collected fully. Since it takes too much time for collection with in-house machine, and which gives worse diffraction, proper amount of data in synchrotron were collected.

For 2065308, the majority of I2, I3, and I5 could be refined at the specific position. Even though their I2, I3, and I5 occupancy is slightly low, but the crystal structure is worth being on the evidence for Pd_3L_2 assembly, supporting that anion exchange triggers structural transformation from Pd_6L_8 to Pd_3L_2, and a trace of bromide is remained from starting materials.

For 2065309 and 2096698, even though we tried several times to mount the crystals, present data set showed the best result. The crystal was highly air-sensitive and diffracted very weakly especially at higher diffraction angles, which is most likely related to large void volume occupied by disordered solvent molecules. As a result, the crystal quality and data were not good enough, so a sufficient fraction of the unique data is above the 2 sigma level. After several attempt of data collection, the reported one is found as the best. The data were collected in 3rd generation synchrotron beamline which is suitable for small molecules' structures. However, the extremely poor scattering power of the crystals does not allow for higher order data to be collected.

Solvate molecules which are squeezed out were calculated by TG, elemental analyses.

Table S1. Crystallographic data of $[Pd_3Cl_6L_2]\cdot 3C_4H_8O_2\cdot 3DMF$, $[Pd_3Br_6L_2]\cdot 2C_4H_8O_2\cdot 5DMF$, $[Pd_3I_6L_2]\cdot C_4H_8O_2\cdot 2DMF\cdot 3CH_2I_2$, $[Pd_3I_6L_2]\cdot 4Me_2SO\cdot MeOH$, $[Pd_6L_8]^{12+}(BF_4^-)_{12}\cdot 13THF\cdot 7Me_2SO$, and $[Pd_6L_8]^{12+}(CF_3SO_3^-)_{12}\cdot 15THF\cdot 4Me_2SO$

	$[Pd_3Cl_6L_2]\cdot 3C_4H_8O_2\cdot 3DMF$	$[Pd_3Br_6L_2]\cdot 2C_4H_8O_2\cdot 5DMF$	$[Pd_3I_6L_2]\cdot C_4H_8O_2\cdot 2DMF\cdot 3CH_2I_2$
Empirical formula	$C_{210}\ H_{210}\ Cl_{12}\ N_{30}\ O_{42}\ Pd_6$	$C_{107}\ H_{111}\ Br_6\ N_{17}\ O_{21}\ Pd_3$	$C_{97}\ H_{88}\ I_{12}\ N_{14}\ O_{16}\ Pd_3$
Formula weight	4889.87	2769.78	3547.81
Temperature (K)	173(2)	173(2) K	173(2) K
Wavelength (Å)	0.71073	0.71073 Å	0.630 Å
Crystal system	Monoclinic	Monoclinic	Triclinic
Space group	$P2_1$	$P2_1$	P-1
a (Å)	14.312(3)	14.785(3)	17.007(3)
b (Å)	25.965(5)	26.130(5)	18.398(4)
c (Å)	15.502(3)	15.368(3)	21.837(4)
α (°)	-	-	90.09(3)
β (°)	107.69(3)	108.44(3)	107.51(3)
γ (°)	-	-	116.28(3)
Volume (Å^3)	5488(2)	5632(2)	5769(3)
Z	1	2	2
Density (calculated) (Mg/m^3)	1.479	1.633	2.042
Absorption coefficient (mm^{-1})	0.707	2.677	2.666
F(000)	2496	2776	3340
Crystal size (mm^3)	0.250 x 0.250 x 0.180	0.220 x 0.200 x 0.160	0.126 x 0.114 x 0.082
Theta range for data collection	3.089 to 26.372	3.008 to 24.712	1.518 to 25.000
Index ranges	-17<=h<=17, -32<=k<=32, -19<=l<=19	-17<=h<=17, -30<=k<=30, -17<=l<=18	-22<=h<=22, -24<=k<=24, -29<=l<=29
Reflections collected	46129	40983	54102
Independent reflections	21975 [R(int) = 0.0568]	19136 [R(int) = 0.0779]	27313 [R(int) = 0.0355]
Completeness to theta	99.50%	99.60%	94.70%
Absorption correction	Semi-empirical from equivalents	Semi-empirical from equivalents	Empirical
Max. and min. transmission	1.000 and 0.789	1.0000 and 0.5020	1.000 and 0.789
Refinement method	Full-matrix least-squares on F^2	Full-matrix least-squares on F^2	Full-matrix least-squares on F^2
Data / restraints / parameters	21975 / 2598 / 1582	19136 / 1911 / 1111	27313 / 992 / 1504
Goodness-of-fit on F^2	0.979	1.016	1.074
Final R indices [I>2sigma(I)]	R1 = 0.0606, wR2 = 0.1160	R1 = 0.0703, wR2 = 0.1705	R1 = 0.0848, wR2 = 0.2644
R indices (all data)	R1 = 0.1070, wR2 = 0.1317	R1 = 0.1244, wR2 = 0.1935	R1 = 0.1435, wR2 = 0.2971
Absolute structure parameter	0.07(3)	0.478(17)	-
Largest diff. peak and hole (e.Å^{-3})	0.915 and -0.453	1.243 and -0.532	3.521 and -1.961
CCDC No.	2065305	2065306	2065307

Table S1. (*Continued*)

	$[Pd_3I_6L_2]\cdot 4Me_2SO\cdot MeOH$	$[Pd_6L_8]^{12+}(BF_4^-)_{12}\cdot 13THF \cdot 7Me_2SO$	$[Pd_6L_8]^{12+}(CF_3SO_3^-)_{12}\cdot 15THF \cdot 4Me_2SO$
Empirical formula	$C_{93}\ H_{88}\ I_6\ N_{12}\ O_{17}\ Pd_3\ S_4$	$C_{402}\ H_{386}\ B_{12}\ F_{48}\ N_{48}\ O_{68}\ Pd_6\ S_7$	$C_{416}\ H_{384}\ F_{36}\ N_{48}\ O_{103}\ Pd_6\ S_{16}$
Formula weight	2854.59	8882.11	9539.05
Temperature (K)	173(2)	100(2)	103(2)
Wavelength (Å)	0.71073	0.850	0.900
Crystal system	Monoclinic	Cubic	Tetragonal
Space group	$P2_1/n$	$Pn\text{-}3n$	$P4/nnc$
a (Å)	17.2568(7)	31.903(4)	31.691(4)
b (Å)	22.2766(9)	-	-
c (Å)	25.6771(11)	-	31.686(6)
β (°)	93.894(3)	-	-
Volume ($Å^3$)	9848.1(7)	32472(11)	31823(11)
Z	4	2	2
Density (calculated) (Mg/m^3)	1.925	0.908	0.996
Absorption coefficient (mm^{-1})	2.579	0.380	0.536
F(000)	5544	9116	9792
Crystal size (mm^3)	0.180 x 0.170 x 0.100	0.100 x 0.070 x 0.040	0.070 x 0.070 x 0.050
Theta range for data collection	1.379 to 24.999	1.870 to 30.494	1.151 to 24.349
Index ranges	-20<=h<=20, -26<=k<=26, -30<=l<=30	-37<=h<=37, -34<=k<=34, -37<=l<=37	-28<=h<=28, -28<=k<=28, -28<=l<=28
Reflections collected	148236	166588	91789
Independent reflections	17336 [R(int) = 0.1785]	4833 [R(int) = 0.1746]	6572 [R(int) = 0.1546]
Completeness to theta	99.90%	99.60%	99.00%
Absorption correction	Semi-empirical from equivalents	Empirical	Empirical
Max. and min. transmission	1.000 and 0.789	1.000 and 0.899	1.000 and 0.902
Refinement method	Full-matrix least-squares on F^2	Full-matrix least-squares on F^2	Full-matrix least-squares on F^2
Data / restraints / parameters	17336 / 492 / 1135	4833 / 1094 / 296	6572 / 839 / 488
Goodness-of-fit on F^2	1.033	1.573	1.389
Final R indices [I>2sigma(I)]	R1 = 0.0693, wR2 = 0.1696	R1 = 0.2070, wR2 = 0.4881	R1 = 0.1578, wR2 = 0.3837
R indices (all data)	R1 = 0.1497, wR2 = 0.2121	R1 = 0.2902, wR2 = 0.5498	R1 = 0.2314, wR2 = 0.4487
Largest diff. peak and hole ($e.Å^{-3}$)	1.574 and -1.259	1.510 and -1.592	1.264 and -0.939
CCDC No.	2065308	2065309	2096698

Table S2. Selected bond length and angles of $[Pd_3Cl_6L_2]\cdot 3C_4H_8O_2\cdot 3DMF$, $[Pd_3Br_6L_2]\cdot 2C_4H_8O_2\cdot 5DMF$, $[Pd_3I_6L_2]\cdot C_4H_8O_2\cdot 2DMF\cdot 3CH_2I_2$, $[Pd_3I_6L_2]\cdot 4Me_2SO\cdot MeOH$, $[Pd_6L_8]^{12+}(BF_4^-)_{12}\cdot 13THF\cdot 7Me_2SO$, and $[Pd_6L_8]^{12+}(CF_3SO_3^-)_{12}\cdot 15THF\cdot 4Me_2SO$

$[Pd_3Cl_6L_2]\cdot 3C_4H_8O_2\cdot 3DMF$		**$[Pd_3Br_6L_2]\cdot 2C_4H_8O_2\cdot 5DMF$**		**$[Pd_3I_6L_2]\cdot C_4H_8O_2\cdot 2DMF\cdot 3CH_2I_2$**		**$[Pd_3I_6L_2]\cdot 4Me_2SO\cdot MeOH$**	
Pd11-N13	2.009(7)	Pd11-N14	1.983(8)	Pd(1)-N(17B)	2.014(7)	Pd(1)-N(7)	2.018(8)
Pd11-N14	2.032(7)	Pd11-N13	1.991(9)	Pd(1)-N(17A)	2.024(8)	Pd(1)-N(1)	2.027(8)
Pd11-Cl12	2.286(3)	Pd11-Br42	2.413(3)	Pd(1)-I(2)	2.5993(13)	Pd(1)-I(2^a)	2.5621(15)
Pd11-Cl22	2.296(3)	Pd11-Br52	2.433(3)	Pd(1)-I(1)	2.6022(14)	Pd(1)-I(1)	2.6097(13)
Pd21-N34^a	2.10(2)	Pd21-N34	2.004(8)	Pd(2)-N(33A)	2.007(7)	Pd(2)-N(9)	2.015(8)
Pd21-N33^a	2.105(8)	Pd21-N33	2.016(7)	Pd(2)-N(33B)	2.011(7)	Pd(2)-N(3)	2.016(9)
Pd21-Cl42	2.281(3)	Pd21-Br62	2.413(2)	Pd(2)-I(4)	2.5925(16)	Pd(2)-I(3^a)	2.4978(17)
Pd21-Cl32	2.293(3)	Pd21-Br72	2.442(2)	Pd(2)-I(3)	2.6017(15)	Pd(2)-I(4)	2.6077(14)
Pd31-N53^a	2.113(16)	Pd31-N54	1.981(8)	Pd(3)-N(49B)	2.030(7)	Pd(3)-N(11)	2.007(8)
Pd31-N54^a	2.10(2)	Pd31-N53	2.013(8)	Pd(3)-N(49A)	2.036(7)	Pd(3)-N(5)	2.030(9)
Pd31-Cl62	2.280(3)	Pd31-Br82	2.432(3)	Pd(3)-I(5)	2.5970(13)	Pd(3)-I(5^a)	2.5719(14)
Pd31-Cl52	2.302(4)	Pd31-Br92	2.437(2)	Pd(3)-I(6)	2.5995(15)	Pd(3)-I(6)	2.5925(12)
N13-Pd11-N14	179.2(4)	N14-Pd11-N13	177.8(5)	N(17B)-Pd(1)-N(17A)	171.3(4)	N(7)-Pd(1)-N(1)	178.4(4)
N13-Pd11-Cl12	89.3(3)	N14-Pd11-Br42	89.5(4)	N(17B)-Pd(1)-I(2)	86.3(2)	N(7)-Pd(1)-I(2^a)	92.5(3)
N14-Pd11-Cl12	91.4(3)	N13-Pd11-Br42	91.2(4)	N(17A)-Pd(1)-I(2)	90.9(3)	N(1)-Pd(1)-I(2^a)	88.2(3)
N13-Pd11-Cl22	89.2(3)	N14-Pd11-Br52	89.2(4)	N(17B)-Pd(1)-I(1)	91.6(2)	N(7)-Pd(1)-I(1)	90.1(3)
N14-Pd11-Cl22	90.0(3)	N13-Pd11-Br52	89.9(4)	N(17A)-Pd(1)-I(1)	91.8(3)	N(1)-Pd(1)-I(1)	89.5(3)
Cl12-Pd11-Cl22	178.55(9)	Br42-Pd11-Br52	177.03(11)	I(2)-Pd(1)-I(1)	174.56(5)	I(2^a)-Pd(1)-I(1)	168.27(6)
N34^a-Pd21-N33^a	177.5(9)	N34-Pd21-N33	179.3(5)	N(33A)-Pd(2)-N(33B)	178.6(3)	N(9)-Pd(2)-N(3)	175.3(4)
N34^a-Pd21-Cl42	89.5(7)	N34-Pd21-Br62	89.4(3)	N(33A)-Pd(2)-I(4)	91.0(3)	N(9)-Pd(2)-I(3^a)	89.3(3)
N33^a-Pd21-Cl42	89.8(4)	N33-Pd21-Br62	90.7(3)	N(33B)-Pd(2)-I(4)	89.3(2)	N(3)-Pd(2)-I(3^a)	90.5(3)
N34^a-Pd21-Cl32	90.9(7)	N34-Pd21-Br72	90.3(3)	N(33A)-Pd(2)-I(3)	91.0(3)	N(9)-Pd(2)-I(4)	92.3(3)
N33^a-Pd21-Cl32	89.8(4)	N33-Pd21-Br72	89.6(3)	N(33B)-Pd(2)-I(3)	88.8(2)	N(3)-Pd(2)-I(4)	88.7(3)
Cl42-Pd21-Cl32	179.59(11)	Br62-Pd21-Br72	177.63(11)	I(4)-Pd(2)-I(3)	177.30(4)	I(3^a)-Pd(2)-I(4)	168.88(6)
N54^a-Pd31-N53^a	173.9(10)	N54-Pd31-N53	176.8(5)	N(49B)-Pd(3)-N(49A)	178.0(3)	N(11)-Pd(3)-N(5)	177.4(4)
N54^a-Pd31-Cl62	91.5(10)	N54-Pd31-Br82	88.2(4)	N(49B)-Pd(3)-I(5)	89.6(3)	N(11)-Pd(3)-I(5^a)	86.9(2)
N53^a-Pd31-Cl62	84.0(5)	N53-Pd31-Br82	89.4(3)	N(49A)-Pd(3)-I(5)	89.9(3)	N(5)-Pd(3)-I(5^a)	91.4(3)
N54^a-Pd31-Cl52	87.5(10)	N54-Pd31-Br92	92.2(4)	N(49B)-Pd(3)-I(6)	90.7(3)	N(11)-Pd(3)-I(6)	90.1(2)
N53^a-Pd31-Cl52	96.7(5)	N53-Pd31-Br92	90.5(3)	N(49A)-Pd(3)-I(6)	89.6(3)	N(5)-Pd(3)-I(6)	91.4(3)
Cl62-Pd31-Cl52	175.71(12)	Br82-Pd31-Br92	172.76(10)	I(5)-Pd(3)-I(6)	176.34(5)	I(5^a)-Pd(3)-I(6)	176.04(5)

Table S2. (*Continued*)

$[Pd_6L_8]^{12+}(BF_4^-)_{12}\cdot 13THF\cdot 7Me_2SO$		$[Pd_6L_8]^{12+}(CF_3SO_3^-)_{12}\cdot 15THF\cdot 4Me_2SO$	
Pd(1)-N(2B)	2.049(11)	Pd(1)-N(19)#1	1.920(13)
Pd(1)-N(2B)#1	2.049(11)	Pd(1)-N(19)	1.920(13)
Pd(1)-N(2B)#2	2.049(11)	Pd(1)-N(51)#2	2.071(11)
Pd(1)-N(2B)#3	2.049(11)	Pd(1)-N(51)#3	2.071(11)
Pd(1)-N(2)	2.089(11)	Pd(2)-N(35)	2.039(11)
Pd(1)-N(2)#2	2.089(11)	Pd(2)-N(35)#4	2.039(11)
Pd(1)-N(2)#1	2.089(11)	Pd(2)-N(35)#5	2.039(11)
Pd(1)-N(2)#3	2.089(12)	Pd(2)-N(35)#3	2.039(11)
N(2B)-Pd(1)-N(2B)#1	88.46(16)	N(19)#1-Pd(1)-N(19)	171.0(14)
N(2)-Pd(1)-N(2)#2	86.7(2)	N(19)#1-Pd(1)-N(51)#2	93.6(6)
N(2B)-Pd(1)-N(2)#1	89.4(8)	N(19)-Pd(1)-N(51)#2	86.2(6)
N(2B)#1-Pd(1)-N(2)#1	23.4(6)	N(19)#1-Pd(1)-N(51)#3	86.2(6)
N(2B)#2-Pd(1)-N(2)#1	174.8(8)	N(19)-Pd(1)-N(51)#3	93.6(6)
N(2B)#3-Pd(1)-N(2)#1	95.0(8)	N(51)#2-Pd(1)-N(51)#3	177.8(10)
N(2)-Pd(1)-N(2)#1	86.7(2)	N(35)-Pd(2)-N(35)#4	170.5(12)
N(2)#2-Pd(1)-N(2)#1	152.4(9)	N(35)-Pd(2)-N(35)#5	89.61(10)
N(2)-Pd(1)-N(2)#3	152.4(9)	N(35)#4-Pd(2)-N(35)#5	89.61(10)
N(2)#2-Pd(1)-N(2)#3	86.7(2)	N(35)-Pd(2)-N(35)#3	89.60(10)
N(2)#1-Pd(1)-N(2)#3	86.7(2)	N(35)#4-Pd(2)-N(35)#3	89.61(10)
		N(35)#5-Pd(2)-N(35)#3	170.5(12)

#1 -z+1/2, y, x
#2 z, y, -x+1/2
#3 -x+1/2, y, -z+1/2

#1 x, -y+1/2, -z+3/2
#2 y, x, -z+3/2
#3 y, - x+1/2, z
#4 -x+1/2, -y+1/2, z
#5 -y+1/2, x, z

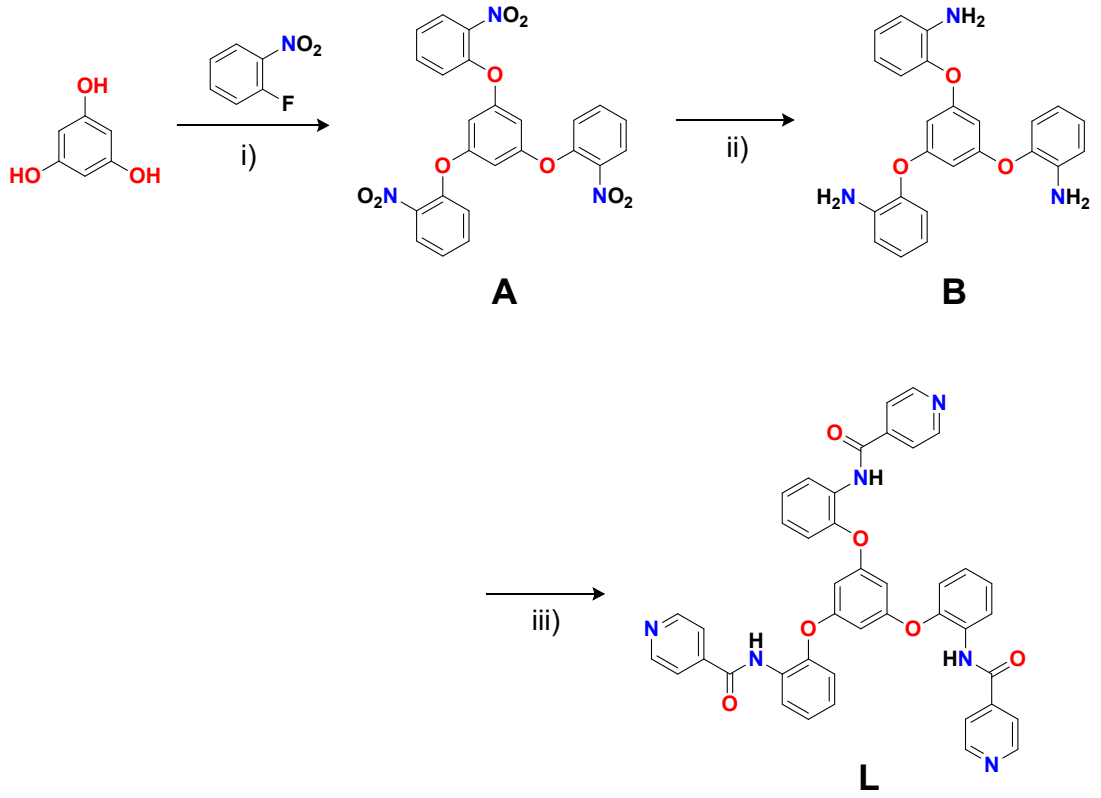

Scheme S1. Synthesis procedure for ligand (L), i) 1-fluoro-2-nitrobenzene, K_2CO_3 in DMF, ii) HCl, Fe powder, KOH in ethanol and iii) isonicotinoyl chloride hydrochloride, triethylamine in $CHCl_3$

Synthesis of 1,3,5-tris(2'-nitrophenoxy)benzene (A)

A mixture of phloroglucinol (1.2 g, 10 mmol), 1-fluoro-2-nitrobenzene (4.65 g, 33 mmol), and potassium carbonate (13.5 g, 90 mmol) in 100 mL of *N,N*-dimethylformamide (DMF) was heated to 120 °C for 1 d. The reaction mixture was then cooled to room temperature and the precipitate was filtered out. 1,3,5-tris(2'-nitrophenoxy)benzene (**A**) was recrystallized in DMF/H_2O (90% yield (4.4 g)). ^{1}H NMR (400 MHz, DMSO-d_6) δ 8.06 (d, J = 8.1 Hz, 3H), 7.73 (d, J = 8.1 Hz, 3H), 7.40 (d, J = 8.4 Hz, 3H), 7.33 (d, J = 8.4 Hz, 3H), 6.59 (s, 3H). ^{13}C NMR (101 MHz, DMSO) δ 158.69, 148.54, 141.65, 135.72, 126.30, 125.65, 122.20, 104.64. HR-ESI-TOF-MS (*m/z*): $[C_{24}H_{15}N_3O_9 + Na^+]^+$ = 512.0704 (calc. 512.0706).

Synthesis of 1,3,5-tris(2'-aminophenoxy)benzene (B)

HCl (0.6 mL concd. HCl in 10 mL of 50% ethanol) was slowly added to a stirred solution of **A** (3.4 g, 7 mmol) and Fe powder (5.6 g, 100 mmol) in 50% ethanol (150 mL), and then stirred at 85°C for 1 d. After the reaction, 15% KOH was added and stirred for 30 min. After the precipitate was filtered off, the solution was concentrated to 30 mL under vacuo and extracted with water and chloroform. The organic layer was dried over $MgSO_4$. After removal of solvent, the residue was dried over under vacuo at 40 °C, which is produced 1,3,5-tris(2'-aminophenoxy)benzene (**B**, 2.5 g, 91%). ^{1}H NMR (400 MHz, DMSO-d_6) δ 6.91 (t, J = 7.6 Hz, 3H), 6.83 (d, J = 8.0 Hz, 3H), 6.78 (d, J = 7.9 Hz, 3H), 6.53 (s, 3H), 6.10 (s, 3H), 4.88 (s, 6H). ^{13}C NMR (101 MHz, DMSO) δ = 160.06, 141.19, 141.00, 125.97, 121.22, 116.92, 116.55, 99.17. HR-ESI-TOF-MS (*m/z*): $[C_{24}H_{21}N_3O_3 + H^+]^+$ = 400.1662 (calc. 400.1661).

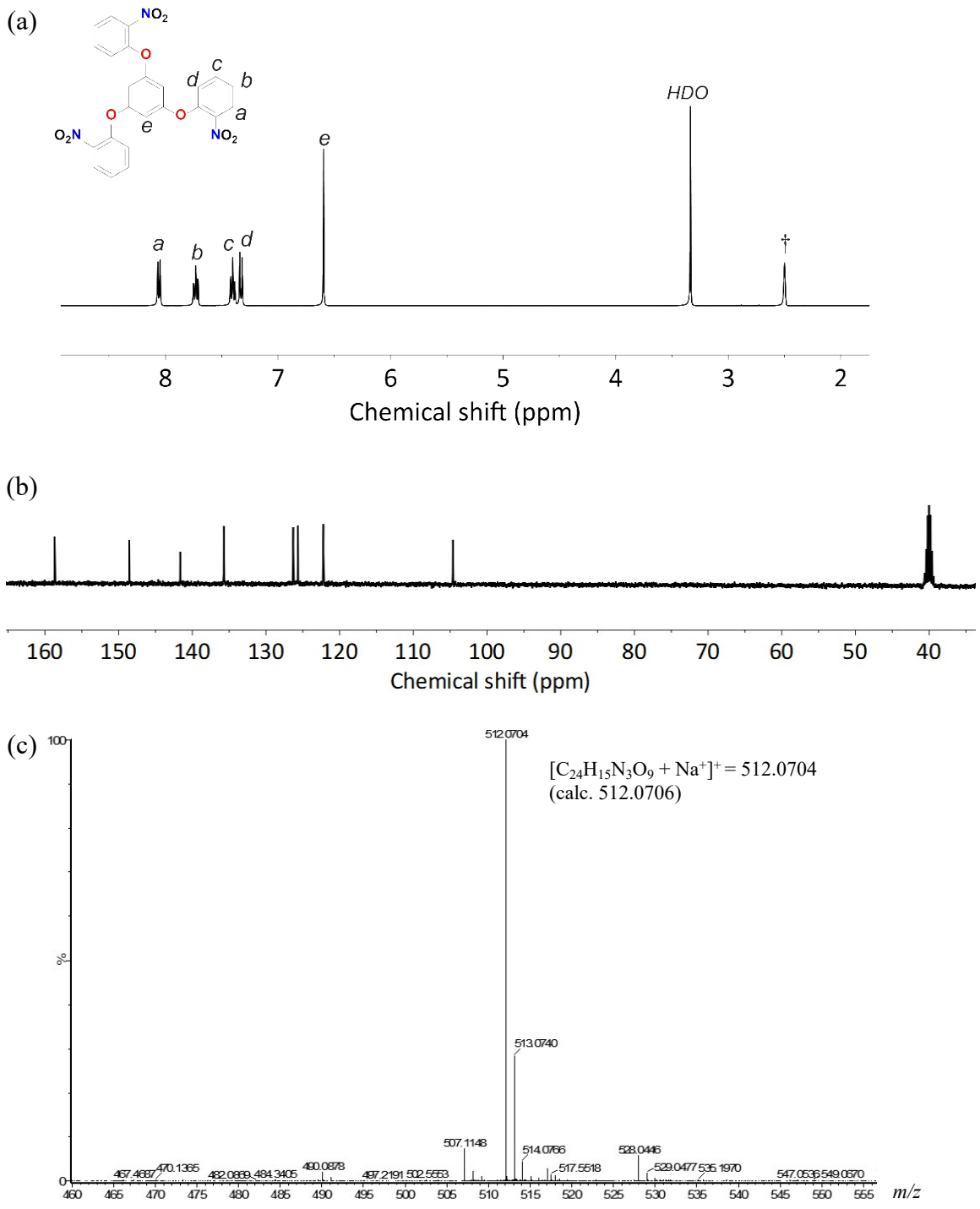

Figure S1. ^{1}H NMR (a), ^{13}C NMR (b), and HR-ESI-Mass (c) spectra for **A** (†: residue of Me_2SO-d_6).

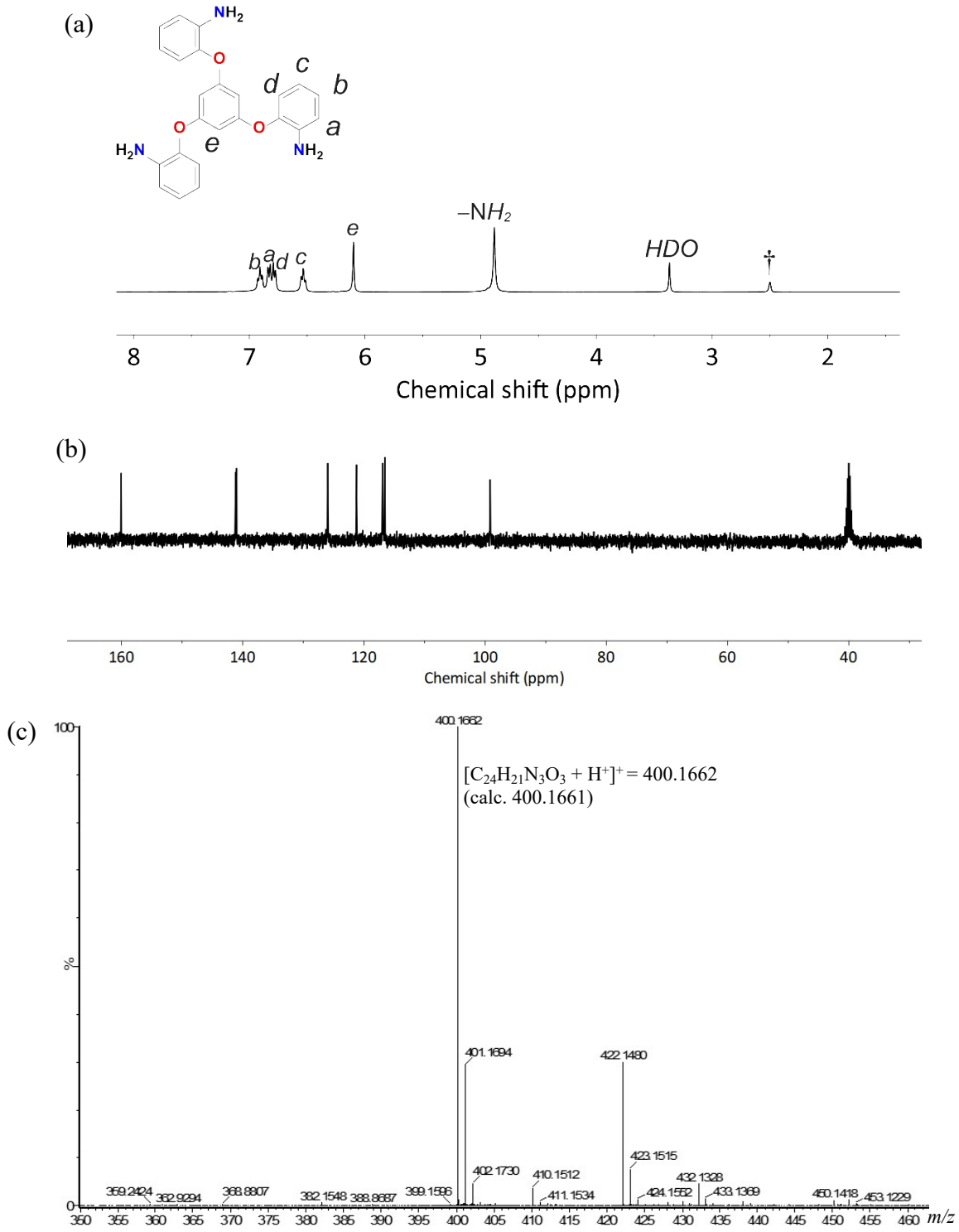

Figure S2. ^{1}H NMR (a), ^{13}C NMR (b), and high resolution ESI-Mass (c) spectra for **B** (†: residue of Me_2SO-d_6).

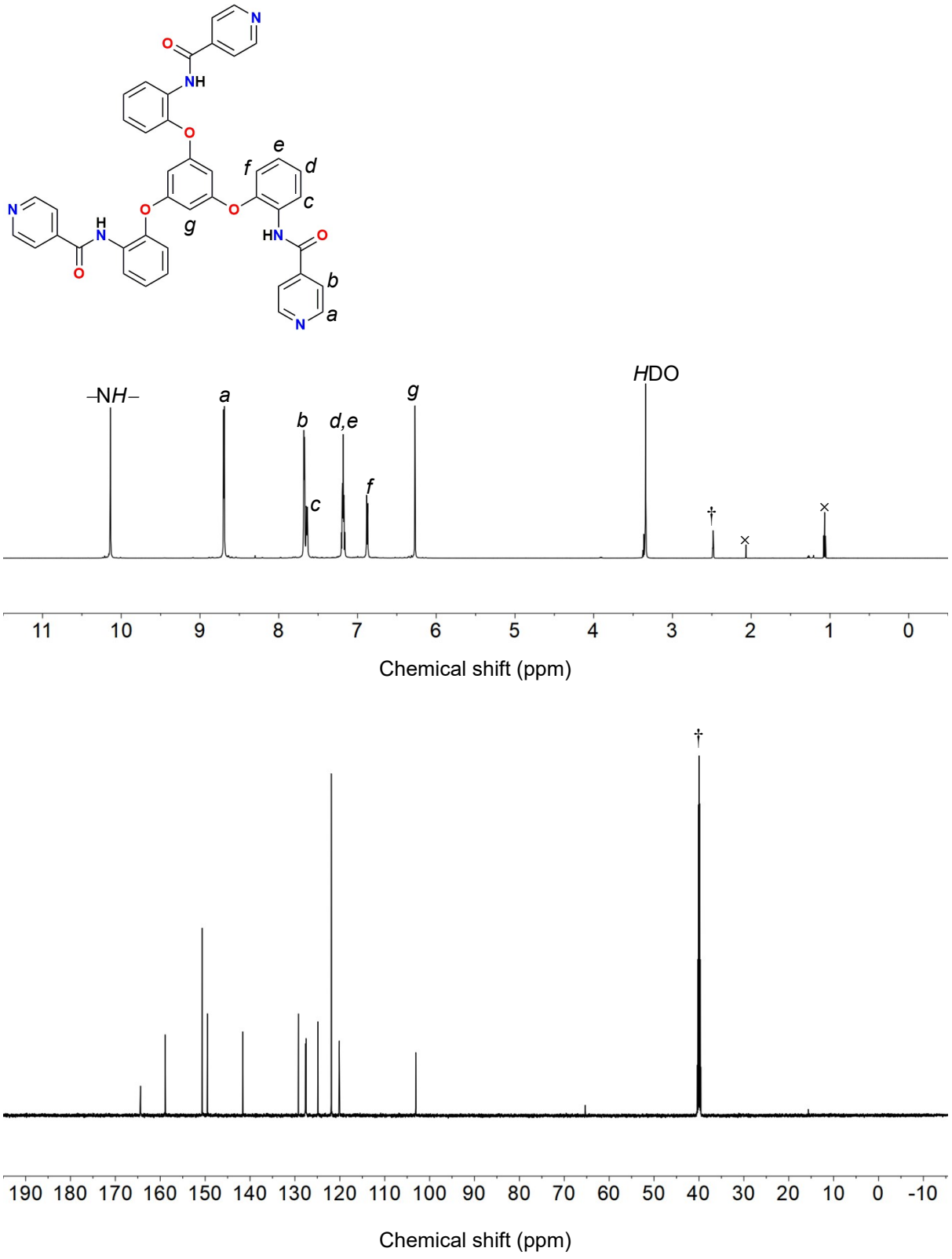

Figure S3. ^{1}H and ^{13}C NMR spectrum for and **L** (†: residue of Me_2SO-d_6).

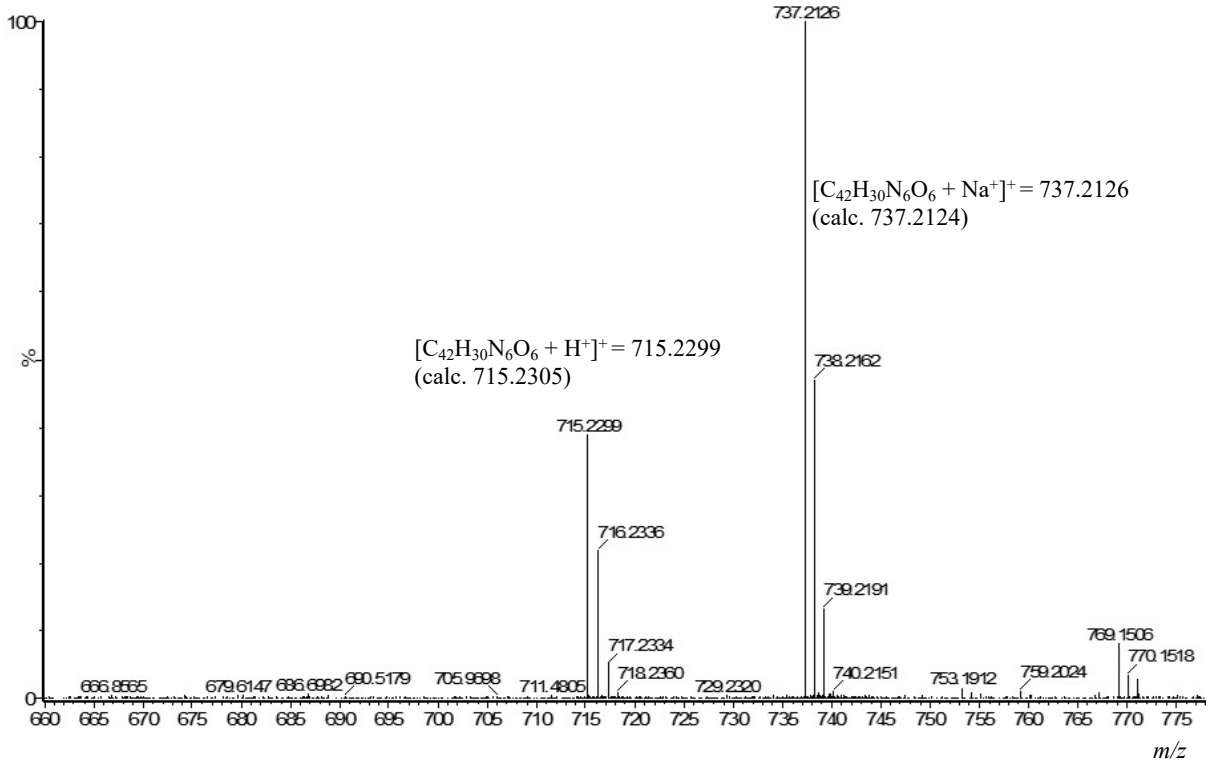

Figure S4. HR-ESI Mass spectrum for **L**.

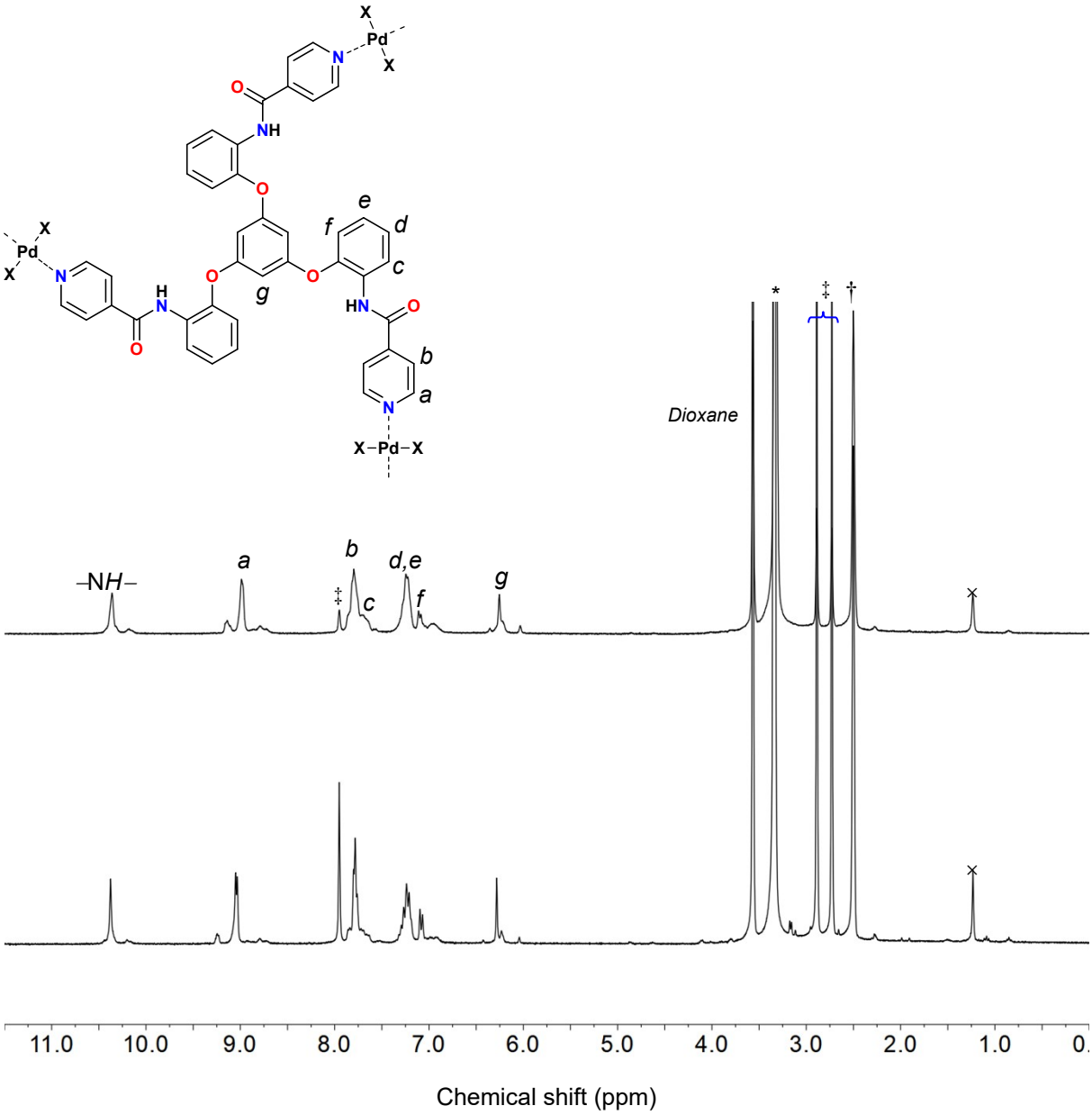

Figure S5. ^{1}H NMR spectra for $[Pd_3Cl_6L_2]\cdot 3C_4H_8O_2\cdot 3DMF$ (top) and $[Pd_3Br_6L_2]\cdot 2C_4H_8O_2\cdot 5DMF$ (bottom) crystalline solids in Me_2SO-d_6 (†: residue of Me_2SO-d_6, *:HDO, ‡:DMF).

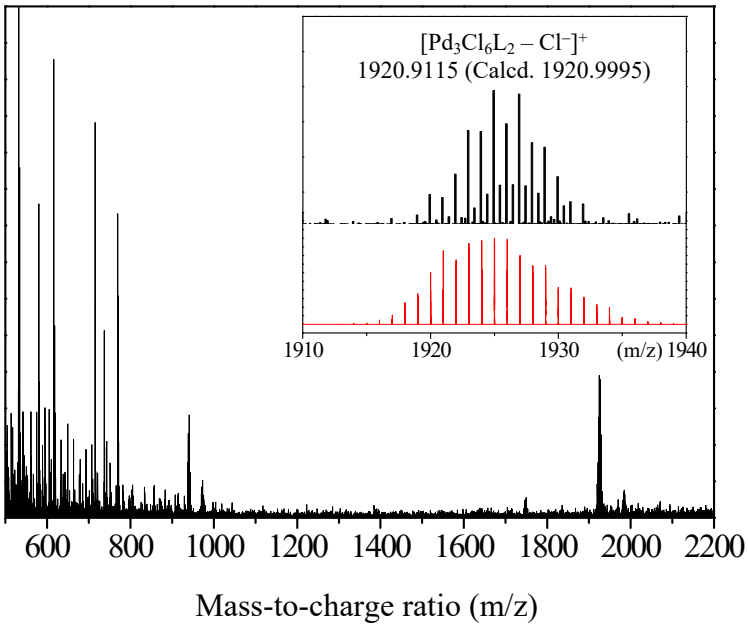

Figure S6. ESI-TOF-Mass spectra (black line, experimental; red line, calculated) for $[Pd_3Cl_6L_2]\cdot 3C_4H_8O_2\cdot 3DMF$.

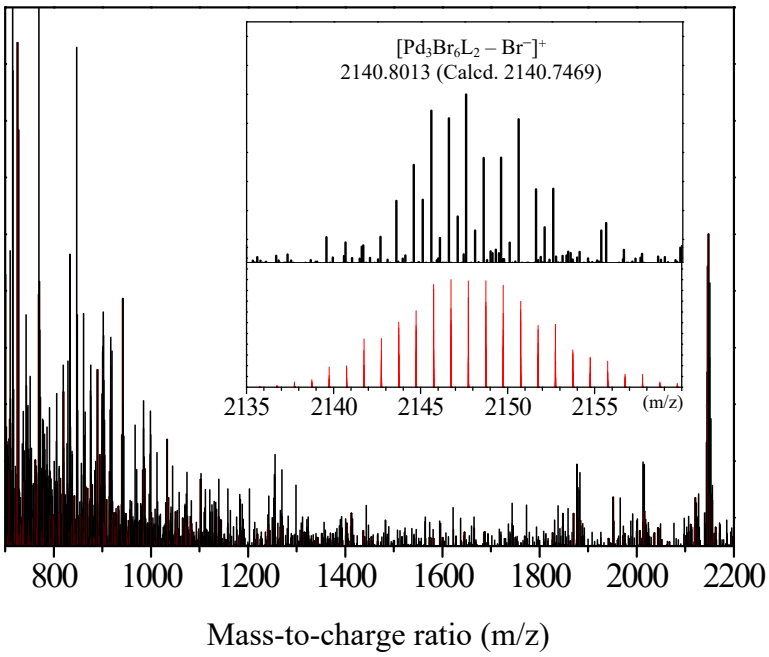

Figure S7. ESI-TOF-Mass spectra (black line, experimental; red line, calculated) for $[Pd_3Br_6L_2]\cdot 2C_4H_8O_2\cdot 5DMF$.

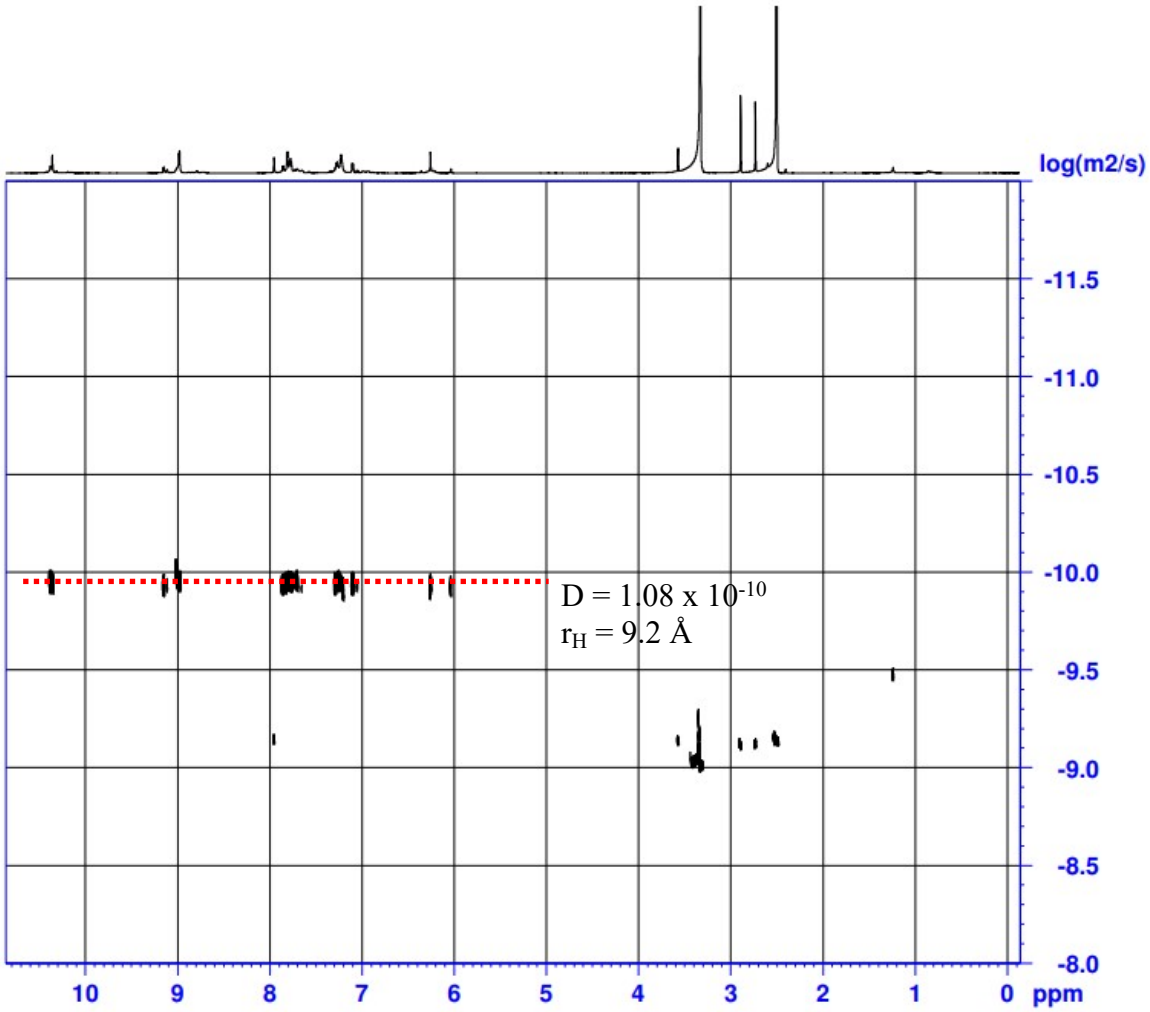

Figure S8. DOSY spectra for $[Pd_3Cl_6L_2]\cdot 3C_4H_8O_2\cdot 3DMF$ in Me_2SO-d_6 at 25 °C.

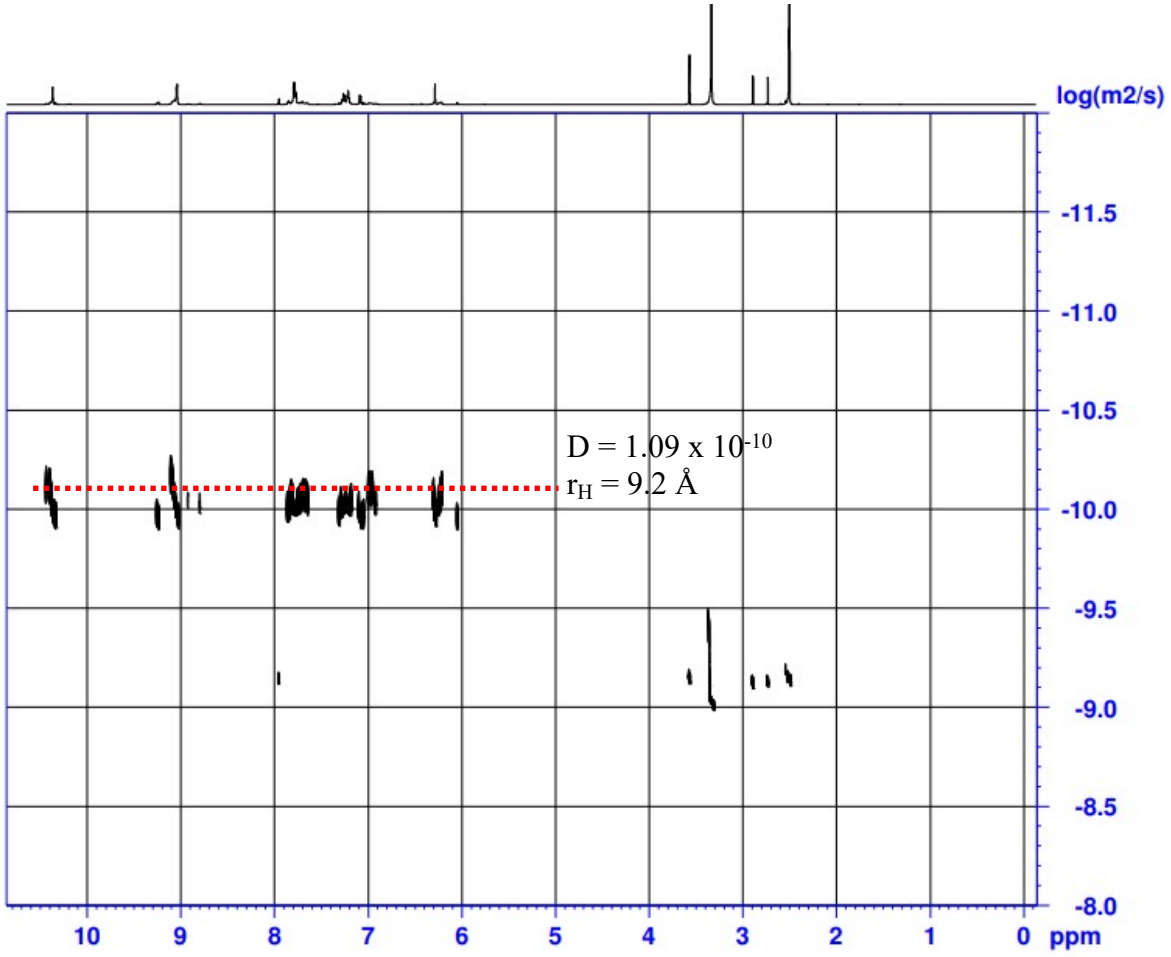

Figure S9. DOSY spectra for $[Pd_3Br_6L_2]\cdot 2C_4H_8O_2\cdot 5DMF$ in Me_2SO-d_6 at 25 °C.

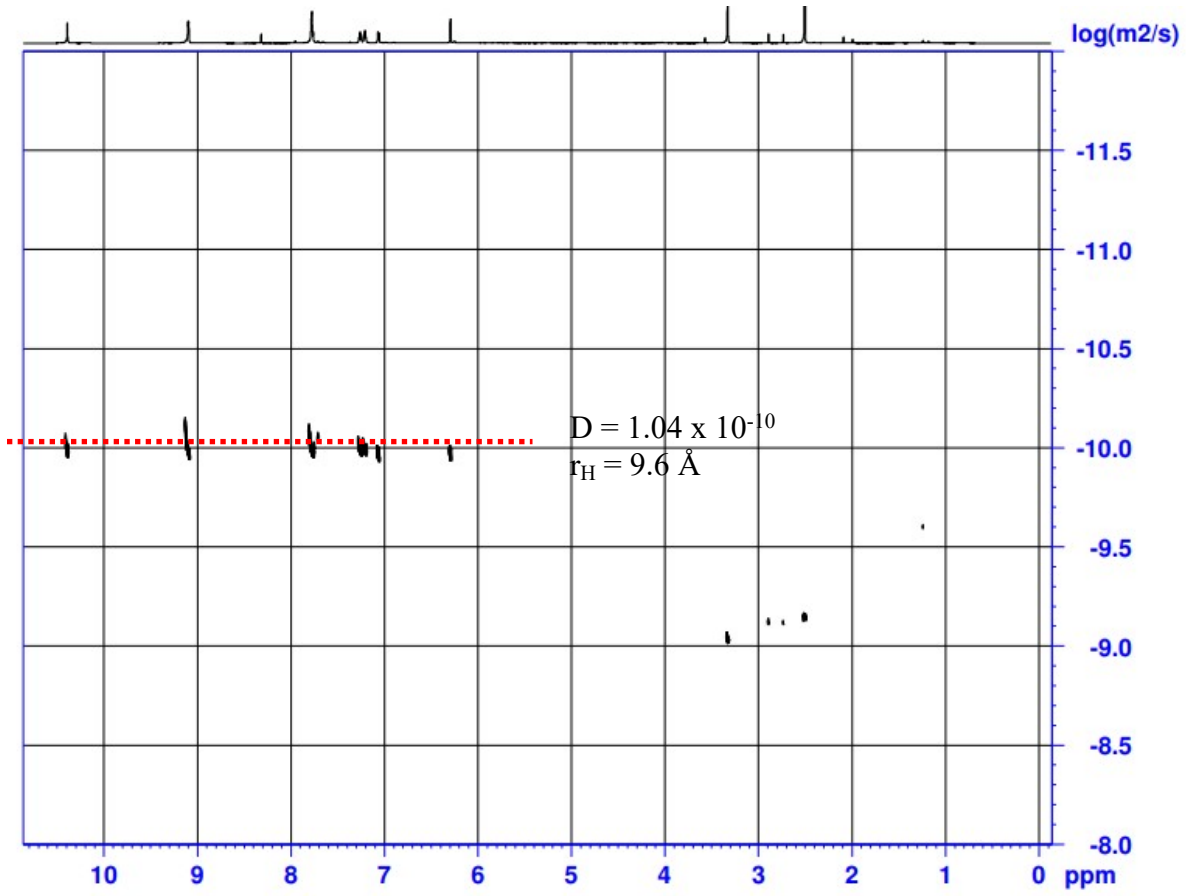

Figure S10. DOSY spectra for $[Pd_3I_6L_2]\cdot C_4H_8O_2\cdot 2DMF\cdot 3CH_2I_2$ in Me_2SO-d_6 at 25 °C.

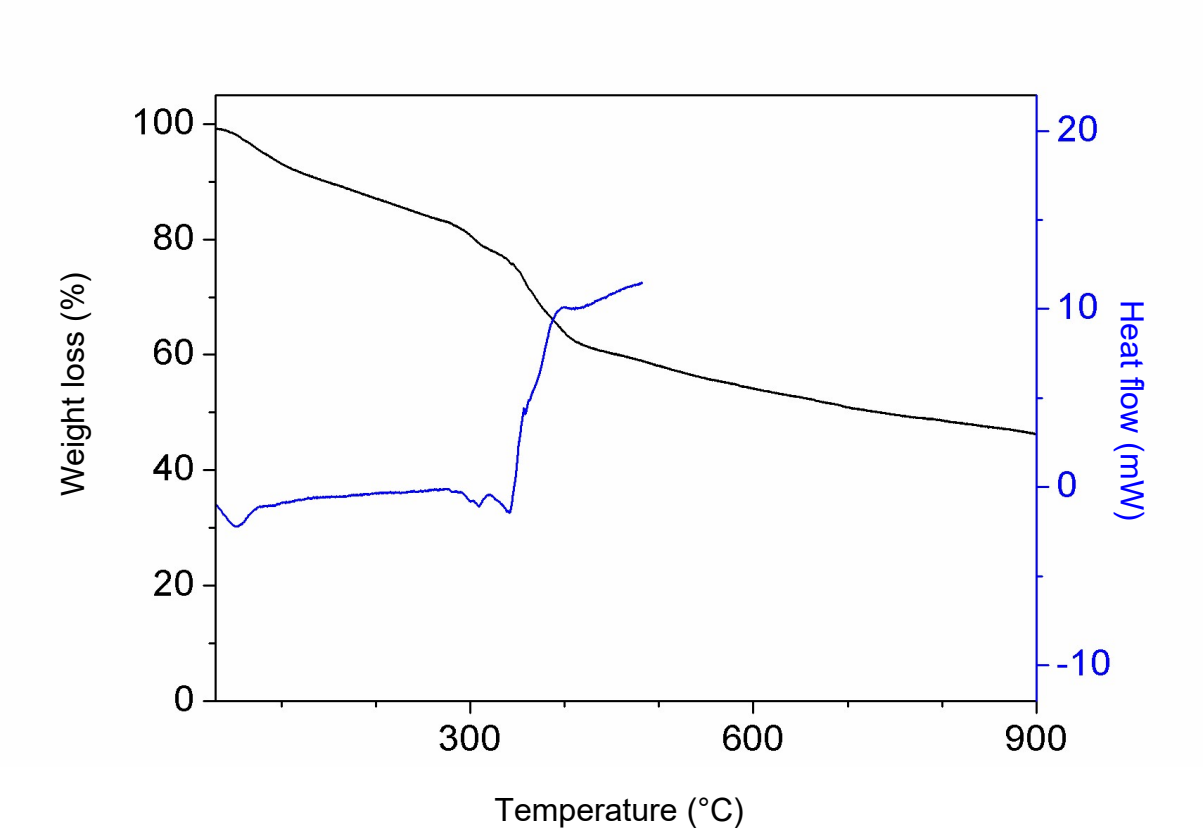

Figure S11. Thermogravimetric analysis for $[Pd_3Cl_6L_2]\cdot 3C_4H_8O_2\cdot 3DMF$, weight loss by solvents: 22.3 % (calcd 19.7%), remain: 46.3 %.

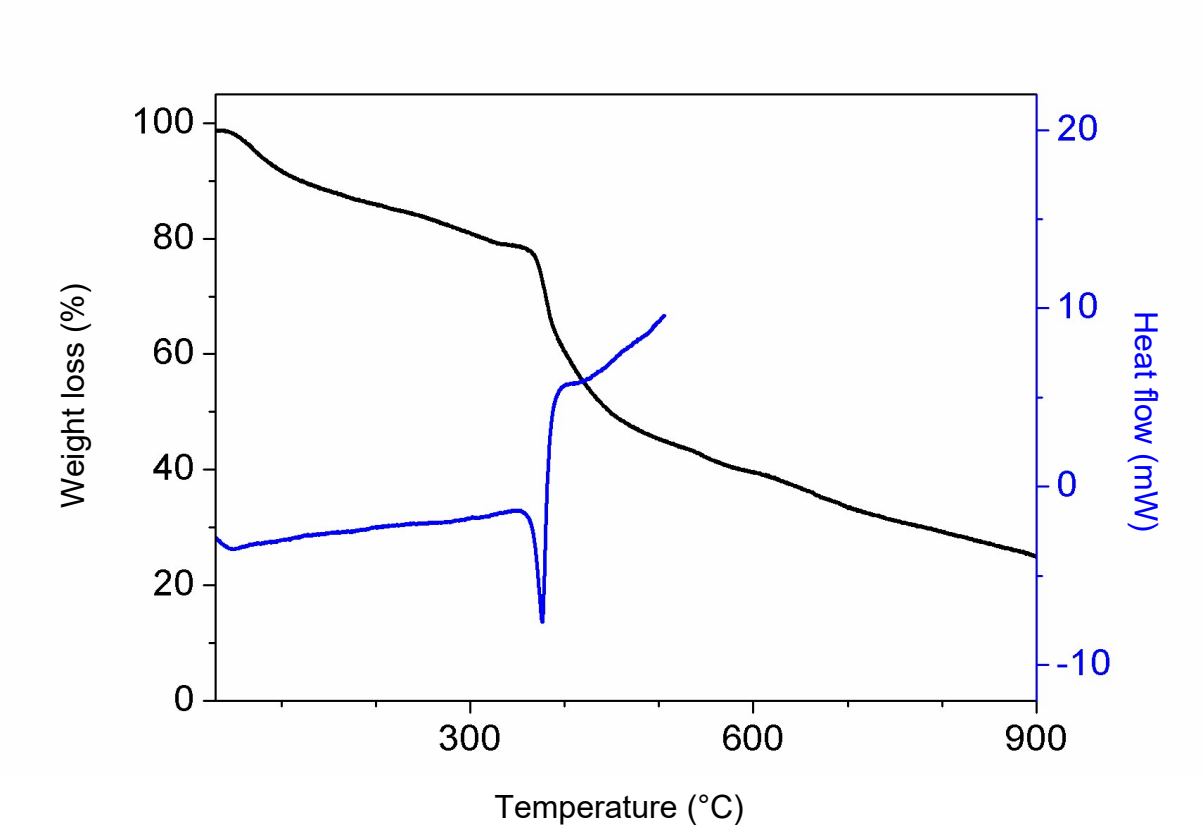

Figure S12. Thermogravimetric analysis for $[Pd_3Br_6L_2]\cdot 2C_4H_8O_2\cdot 5DMF$, weight loss by solvents: 21.6 % (calcd 19.6%), remain: 25.0 %.

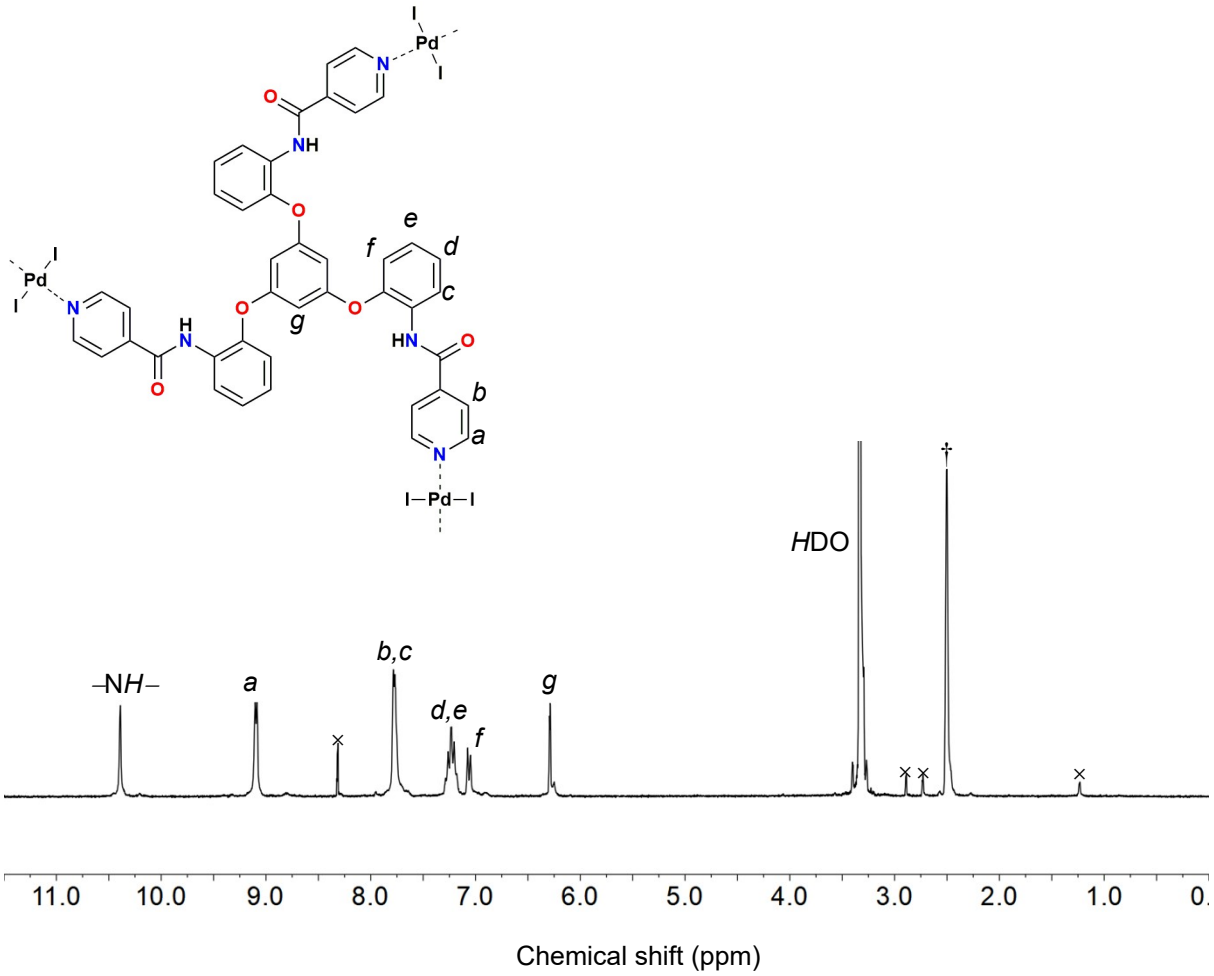

Figure S13. ^{1}H NMR spectrum for $[Pd_3I_6L_2]\cdot C_4H_8O_2\cdot 2DMF\cdot 3CH_2I_2$ (†: residue of Me_2SO-d_6).

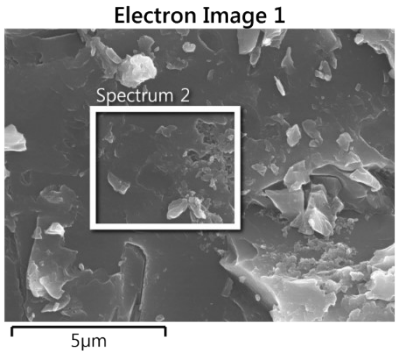

Element	Wt%	Atomic %
C	25.31	54.68
N	9.03	16.73
O	10.20	16.54
Br	0.56	0.18
Pd	16.25	3.96
I	38.66	7.90
Total:		100.00

Figure S14. Energy dispersive X-ray spectroscopy of $[Pd_3I_6L_2]$.

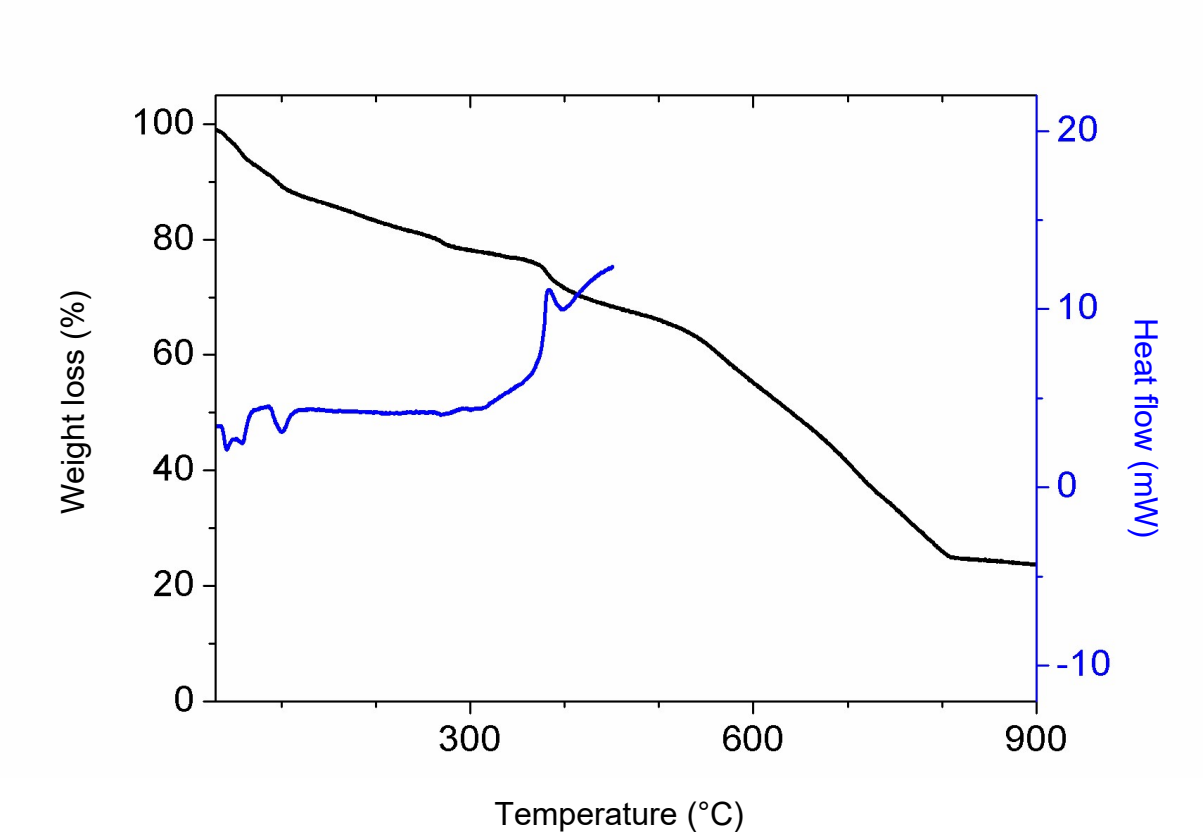

Figure S15. Thermogravimetric analysis for $[Pd_3I_6L_2]\cdot C_4H_8O_2\cdot 2DMF\cdot 3CH_2I_2$, weight loss by solvents: 24.0 % (calcd 29.2%), remain: 24.3 %.

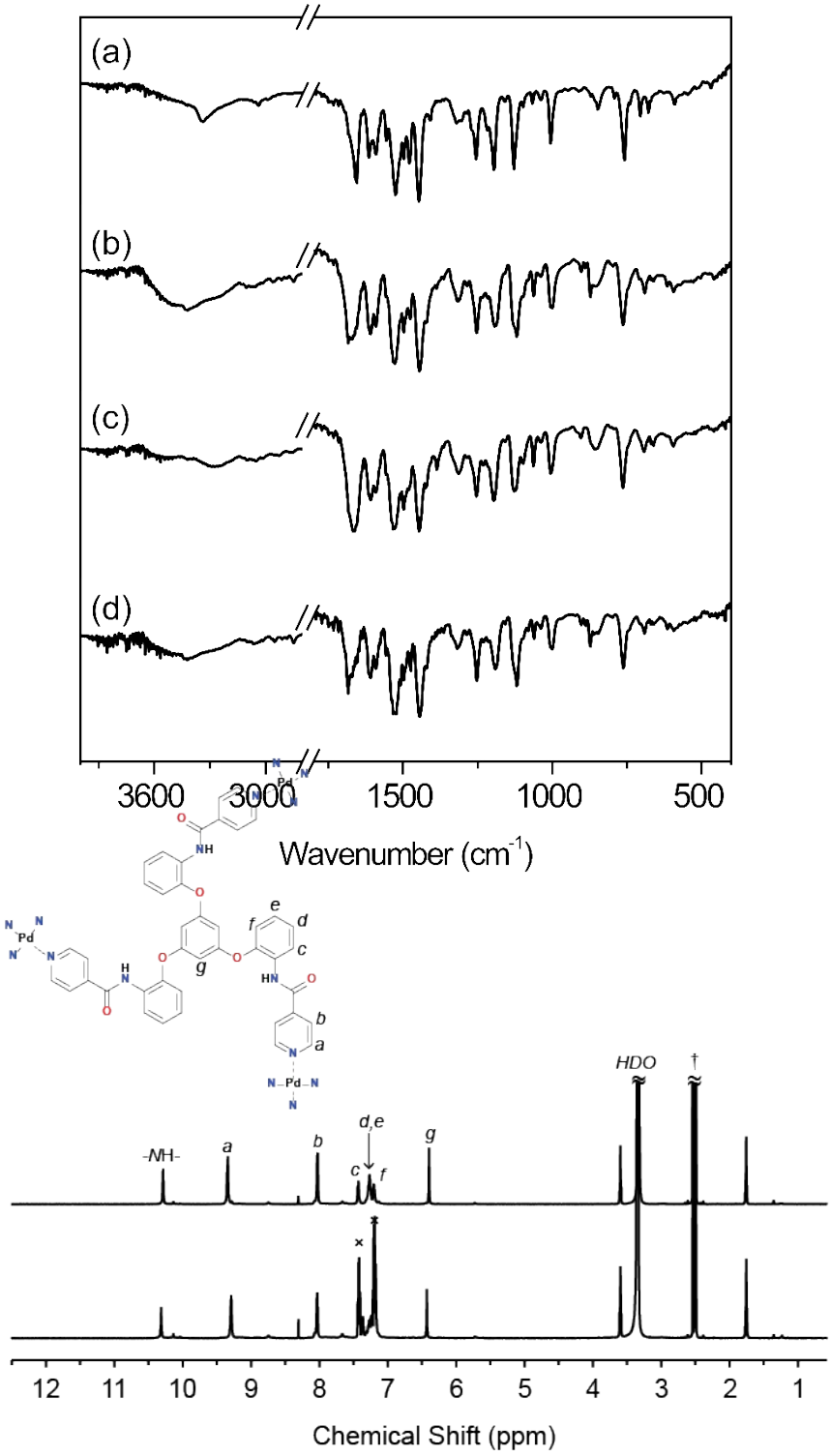

Figure S16. IR spectra for **L** (a), $[Pd_3Cl_6L_2]\cdot 3C_4H_8O_2\cdot 3DMF$ (b), $[Pd_3Br_6L_2]\cdot 2C_4H_8O_2\cdot 5DMF$ (c), and $[Pd_3I_6L_2]\cdot C_4H_8O_2\cdot 2DMF\cdot 3CH_2I_2$ (d).

Figure S17. ^{1}H NMR spectra for $[Pd_6L_8](BF_4)_{12}\cdot 13THF\cdot 7Me_2SO$ (top) and $[Pd_6L_8](CF_3SO_3)_{12}\cdot 15THF\cdot 4Me_2SO$ (bottom) in Me_2SO-d_6 at 25 °C.

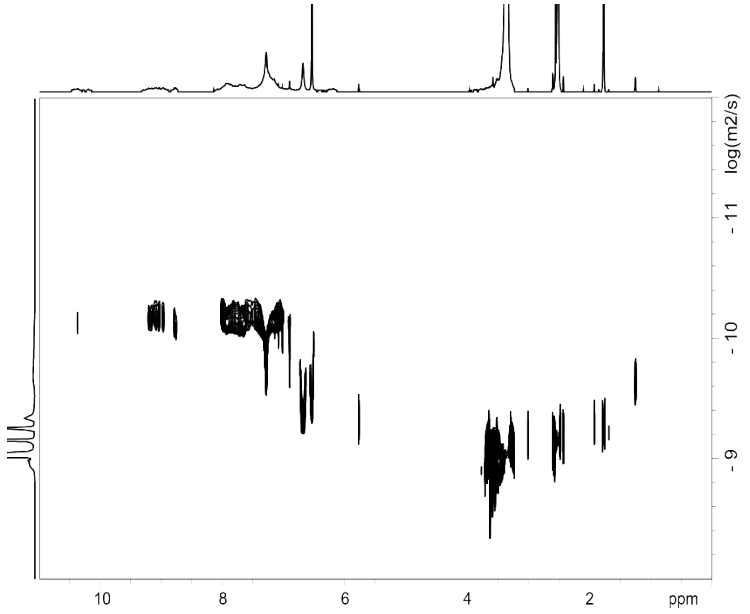

Figure S18. DOSY spectra for $[Pd_6L_8](BF_4)_{12}\cdot 13THF\cdot 7Me_2SO$ in Me_2SO-d_6 at 25 °C, D = 6.43 x 10^{-11}, r_H = 15.5 Å.

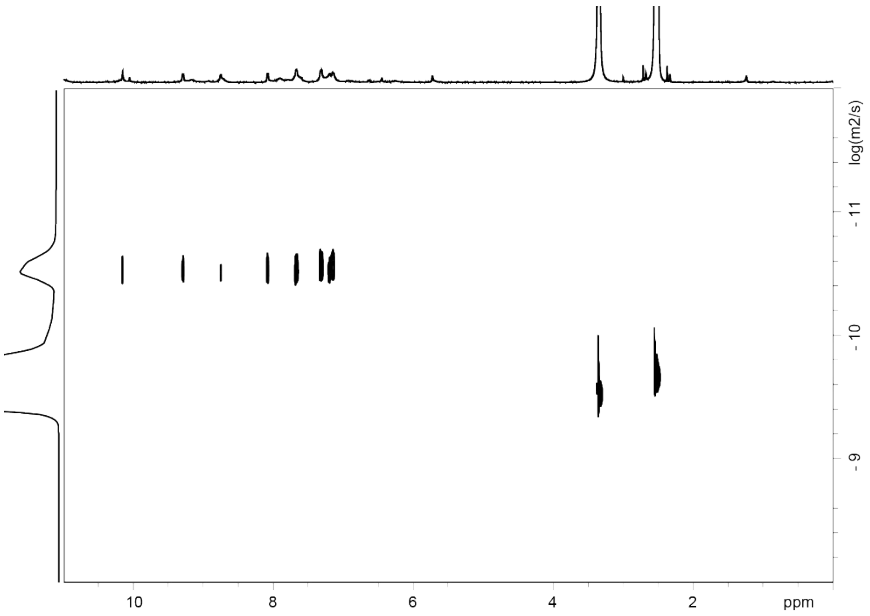

Figure S19. DOSY spectra for $[Pd_6L_8](CF_3SO_3)_{12}\cdot 15THF\cdot 4Me_2SO$ in Me_2SO-d_6 at 25 °C, D = 6.40 x 10^{-11}, r_H = 15.6 Å.

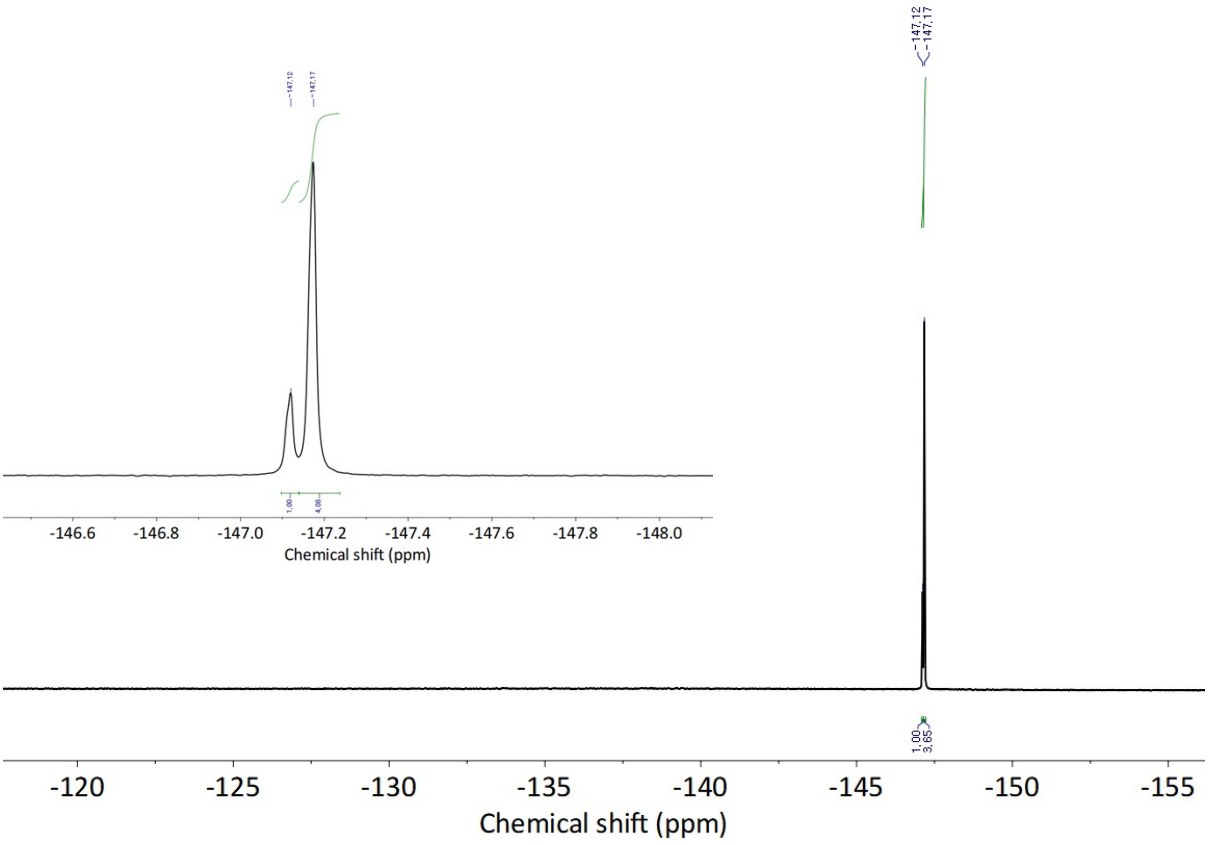

Figure S20. ^{19}F NMR spectra for $[Pd_6L_8](BF_4)_{12}\cdot 13THF\cdot 7Me_2SO$ in Me_2SO-d_6 at 25 °C.

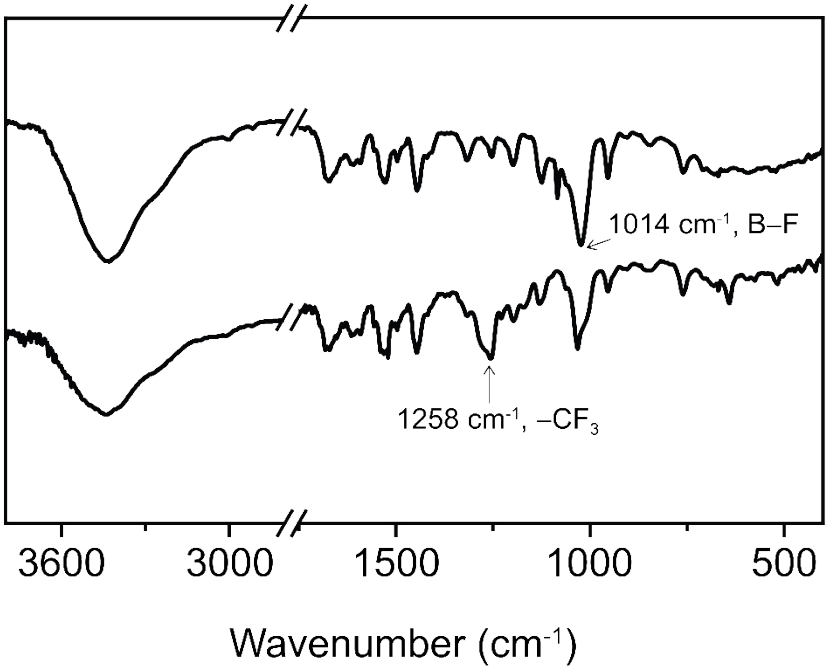

Figure S21. IR spectra for $[Pd_6L_8](BF_4)_{12}\cdot 13THF\cdot 7Me_2SO$ (top) and $[Pd_6L_8](CF_3SO_3)_{12}\cdot 15THF\cdot 4Me_2SO$ (bottom).

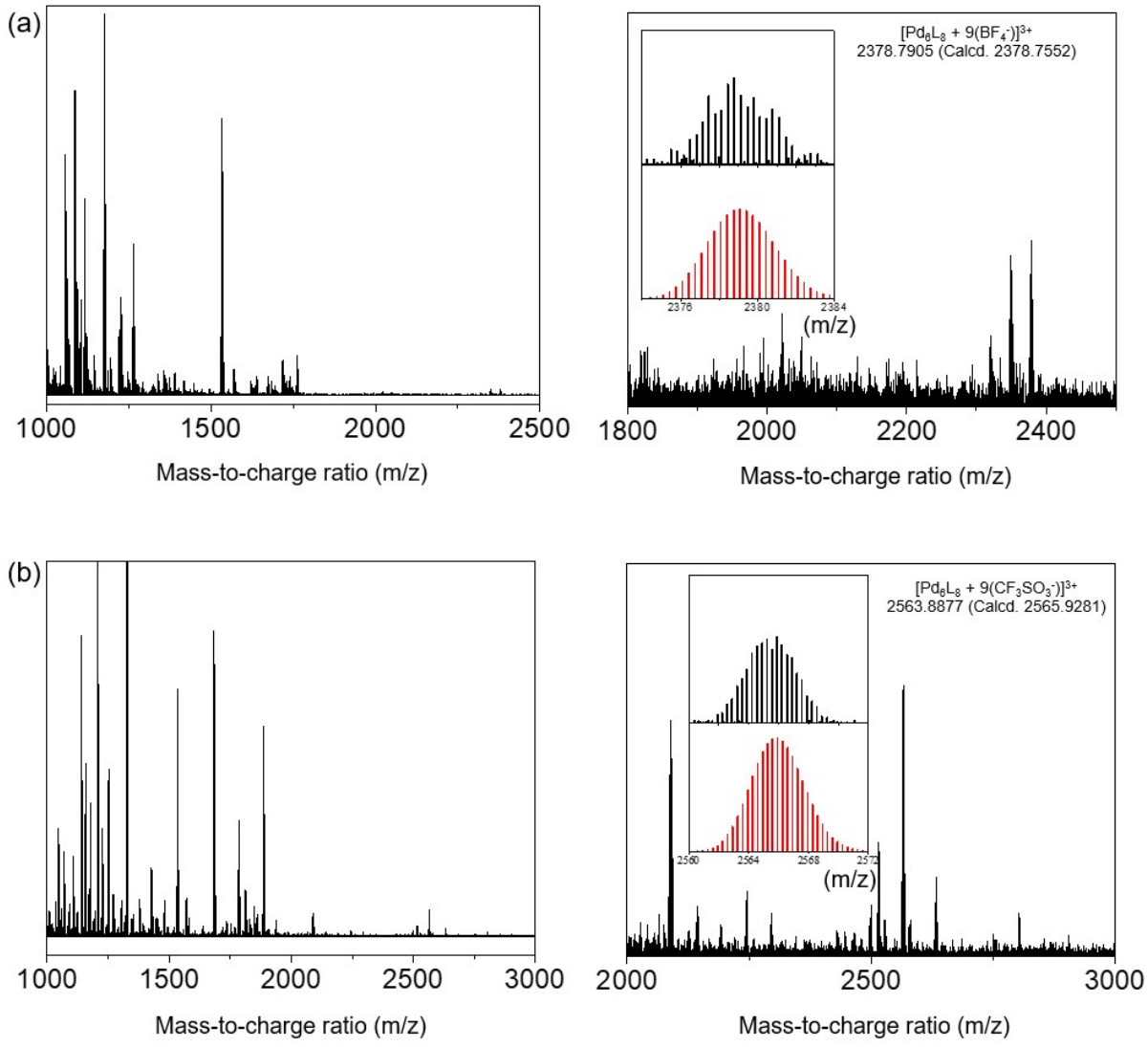

Figure S22. HR-ESI-Mass spectra for $[Pd_6L_8](BF_4)_{12}\cdot 13THF\cdot 7Me_2SO$ (a) and $[Pd_6L_8](CF_3SO_3)_{12}\cdot 15THF\cdot 4Me_2SO$ (b); measured, black; calcd, red.

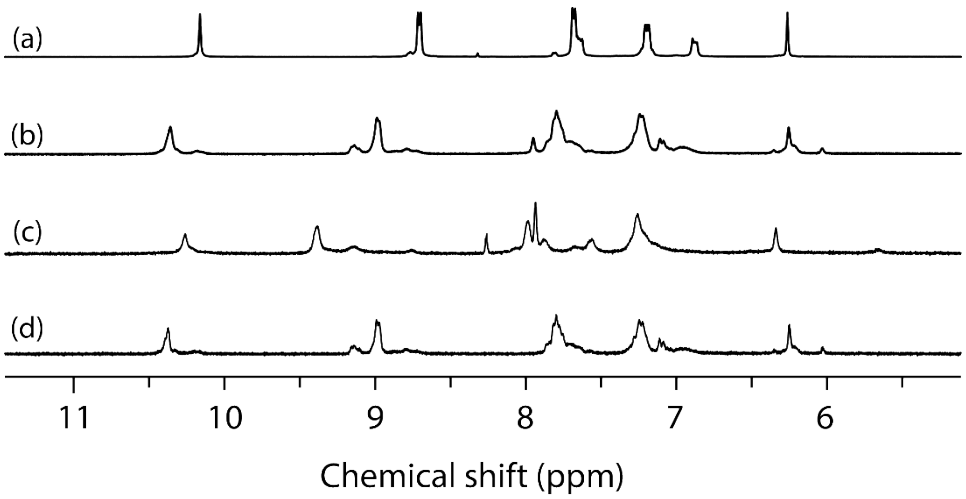

Figure S23. ^{1}H NMR spectra in Me_2SO-d_6 showing structural conversion triggered by anions, (a) L, (b) $[Pd_3Cl_6L_2]$, (c) a sample after the addition of stoichiometric amount of $AgBF_4$ into (b), and (d) the isolated sample and dissolved in Me_2SO-d_6 after the addition of NH_4Cl into (c), the assignment for each peak follows that in Figs. S3 and S5.

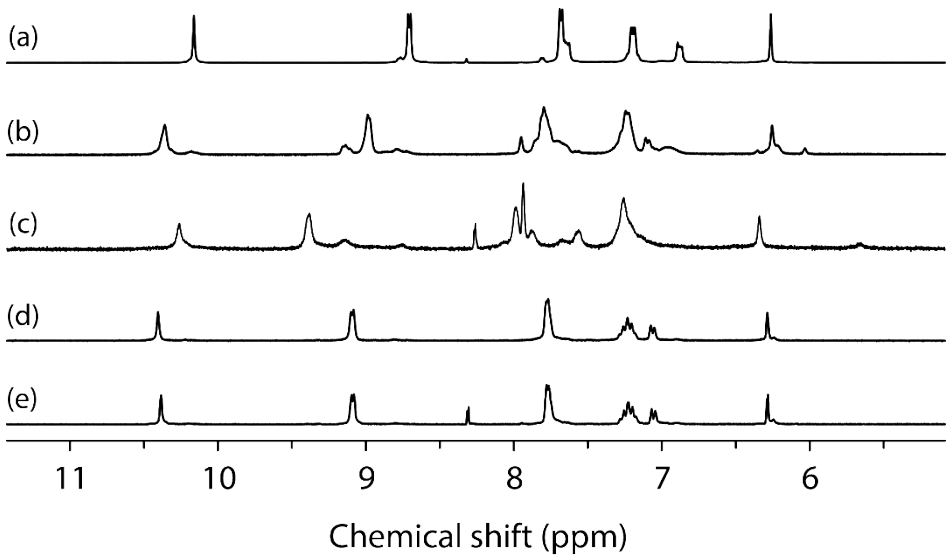

Figure S24. ^{1}H NMR spectra in Me_2SO-d_6 showing structural conversion triggered by anions, (a) L, (b) $[Pd_3Cl_6L_2]$, (c) a sample after the addition of stoichiometric amount of $AgBF_4$ into (b), (d) the isolated sample and dissolved in Me_2SO-d_6 after the addition of NEt_4I into (c), and (e) isolated $[Pd_3I_6L_2]\cdot C_4H_8O_2\cdot 2DMF\cdot 3CH_2I_2$, the assignment for each peak follows in Figs. S3, S5, and S13.

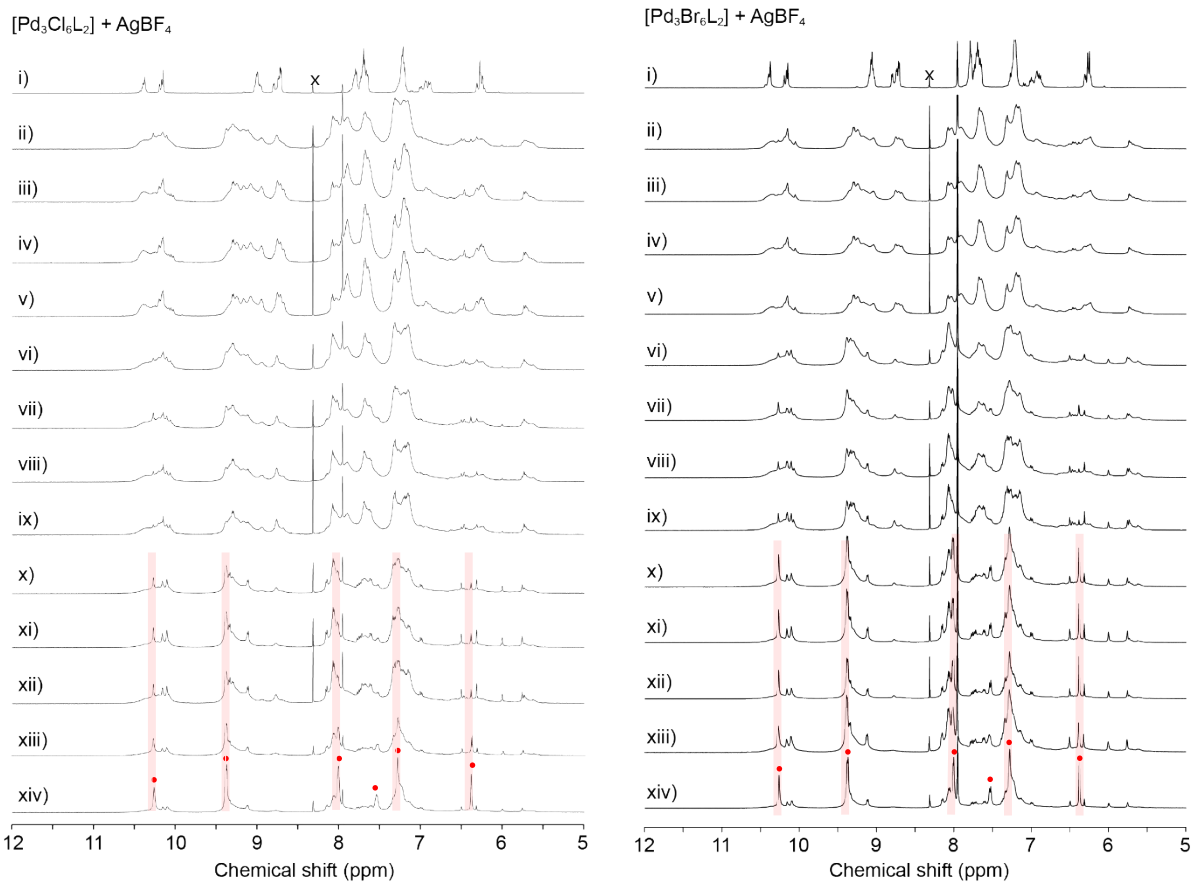

Figure S25. Step wise addition of $AgBF_4$ to $Pd_3Cl_6L_2$ and $Pd_3Br_6L_2$ in Me_2SO-d_6. Each spectrum was obtained in following conditions: i) shows the mixture of $Pd_3X_6L_2$ and L (1:2). ii) was measured after the addition of 0.25 equiv. of $AgBF_4$. The sample was kept at 70 °C iii) for 30 min, iv) for 3 h, and v) for 60 h in total. Spectrum vi) was obtained with the additional 0.25 equiv. of $AgBF_4$ (0.5 equiv. in total). Then the sample was kept vii) at ambiguous temperature for 30 min, viii) heated at 70 °C for 30 min, ix) for 3 hrs.

Then x) was obtained with additional 0.25 equiv. of $AgBF_4$ (0.75 equiv. in total). The sample was kept xi) at ambiguous temperature for 30 min, xii) heated at 70 °C for 1.5 h. xiii) was obtained after the addition of 1 equiv. of $AgBF_4$ in total. xvi) is the spectrum for the sample after heating at 70 °C for 15 h (Red circle: Pd_6L_8 cages' signals).

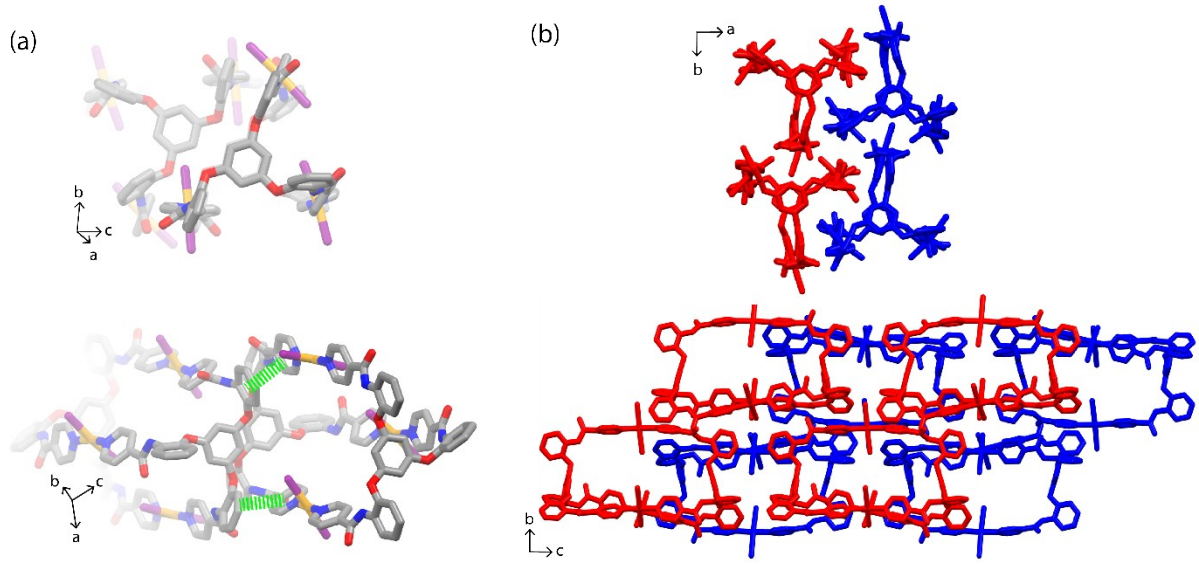

Figure S26. Packing structure of (a) $[Pd_3I_6L_2]\cdot C_4H_8O_2\cdot 2DMF\cdot 3CH_2I_2$ (green dot line indicates stacking between pyridyl and benzene ring) and (b) $[Pd_3I_6L_2]\cdot 4Me_2SO\cdot MeOH$ showing columnar packing in (001) axis (red and blue represent two neighboring columns).

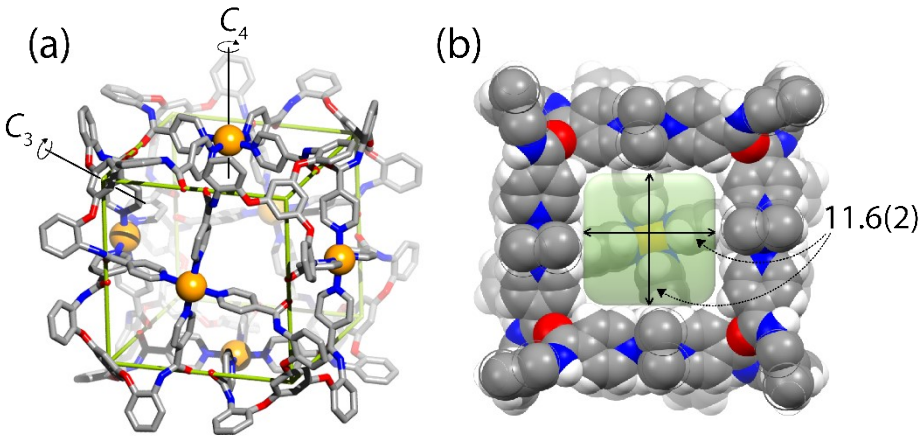

Figure S27. The crystal structure of cube $[Pd_6L_8]^{12+}(BF_4^-)^{12}$ (a) and inner cavity (b).